

DOI: **10.5958/2249-7137.2021.01960.1**

## CHARACTERISTICS OF THE $\text{Fe}_2(\text{MoO}_4)_3 \cdot \text{MoO}_3$ CATALYST USED IN THE SYNTHESIS OF NANOCARBONS FROM METHANE

**Hilola N. Xolmirzayeva\***

Laboratory Assistant,  
Department of Analytical Chemistry,  
Samarkand State University, Samarkand,  
UZBEKISTAN  
Email id: hilola.xolmirzaeva@mail.ru

### ABSTRACT

*The analysis of the physicochemical and operational characteristics of two industrial catalysts for the synthesis of nanocarbon is carried out. Various methods: X-ray phase, chemical, IR spectroscopy investigated the composition of the catalysts. It was shown that the main component of industrial catalysts is iron molybdate (67.27%). The catalyst contains about 31%  $\text{MoO}_3$ , and 1-2% of molybdenum oxide is included in the lattice of iron molybdate, forming a solid solution. The presence of acid sites of the type on the surface of the catalysts was detected by IR spectroscopy. Lewis and Bronsted and the main centres of varying strength. The catalysts are highly active: their formaldehyde productivity reaches a value (12.5-13 mmol/g.s). The surface area of industrial contacts is (7-9  $\text{m}^2/\text{g}$ ); the size of the mesopores is 2-40 nm. Thus, industrial catalysts for the synthesis of nanocarbon are of high quality, which ensures their high performance throughout the entire period of operation.*

**KEYWORDS:** Iron Molybdate, Molybdenum, Catalyst, IR Spectroscopy, Radiograph

### INTRODUCTION

Iron molybdate  $\text{Fe}_2(\text{MoO}_4)_3$  has a monoclinic structure, in which  $\text{Fe}^{3+}$  cations occupy slightly distorted octahedral positions, while  $\text{Mo}^{6+}$  ions have tetrahedral coordination. Both types of ions are linked by an oxygen bridge. The fraction of molybdenum in the form of free  $\text{MoO}_3$  in both industrial Fe - Mo catalysts is about 21% atm in terms of Mo. This is established using X-ray fluorescence analysis. And only a small number of molybdenum atoms (1-2%) are incorporated into the crystal lattice of the  $\text{Fe}_2(\text{MoO}_4)_3$  phase, where there is a significant amount of free

tetrahedral vacancies because only 3 out of 24 available ones are filled. The presence of a significant amount of the free  $\text{MoO}_3$  phase is confirmed by the X-ray phase analysis data, where the diffractograms contain intense reflections of the  $\text{MoO}_3$  phase (Figure 1).

The IR spectra of the studied catalytic systems do not differ significantly, as do the X-ray diffraction patterns for both catalysts. They contain characteristic absorption bands of Mo-O bonds in various compounds. A weak band at  $991\text{ cm}^{-1}$  and broadband at  $624\text{ cm}^{-1}$  characterize the free  $\text{MoO}_3$  phase. The weak and narrowband at  $960\text{ cm}^{-1}$  can be associated with vibrations of the Fe-O-Mo bond. Several broad bands in the range  $700\text{--}900\text{ cm}^{-1}$  can be attributed to tetrahedral Mo species in  $\text{Fe}_2(\text{MoO}_4)_3$  (Fig. 1). The nature of the surface sites of iron-molybdenum oxide catalysts has been studied in several studies [70].

## MATERIALS AND METHODS

These works showed the existence of acid sites and their significant role in the oxidation of methane. However, the results obtained do not allow distinguishing these centres according to type and strength. The performed pK-spectroscopic studies have shown the presence on the surface of the studied samples not only of acidic centres of the Lewis and Bronsted type but also of basic centres.

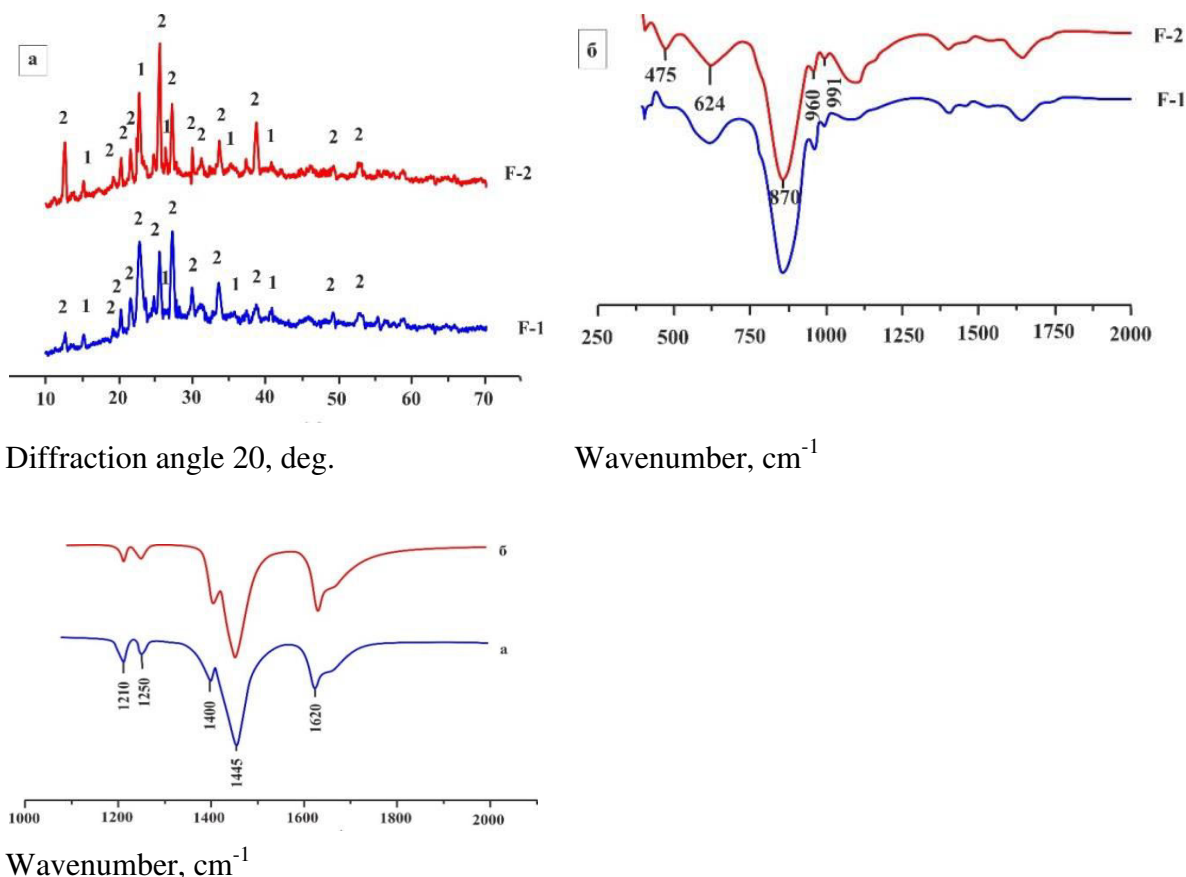


Figure 1.  $\text{Fe}_2(\text{MoO}_4)_3$  (a) and  $\text{Fe}_2(\text{MoO}_4)_3 \cdot \text{MoO}_3$  (b) brand catalyst for nitrogen adsorption and IR spectra

The Lewis acid centre is surface metal cations with free bonds, and the Bronsted acid centre is the Lewis centre that has absorbed water. The main centres are oxygen anions, which are located on the surface. The presence of Lewis centres was confirmed by absorption bands in IR spectra ( $1210$ ,  $1250$ ,  $1620\text{ cm}^{-1}$ ), Bronsted centres ( $1445$ ,  $1400\text{ cm}^{-1}$ ) characterizing coordinated ammonia (Figure 1).

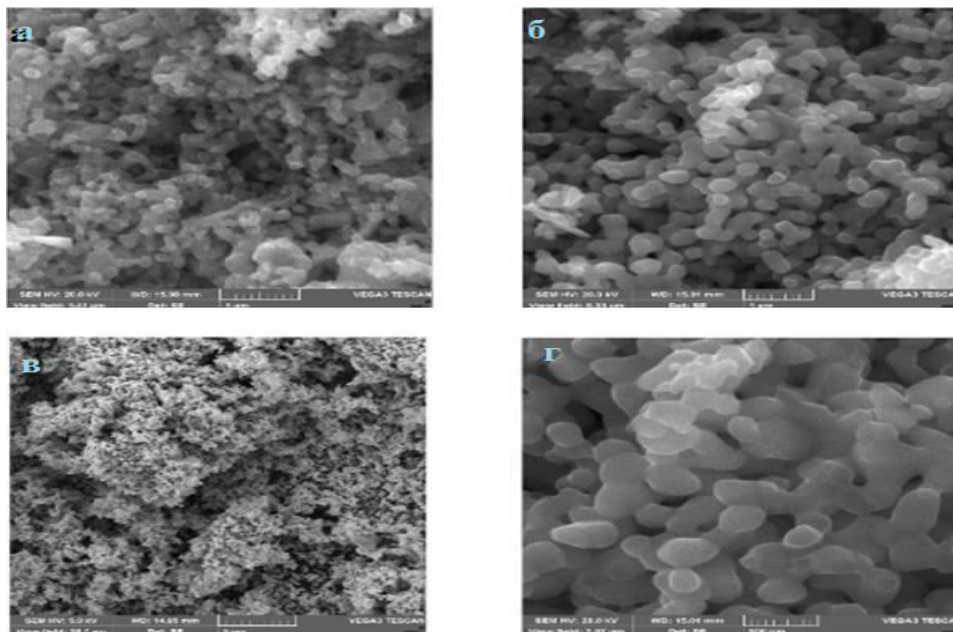


Figure 2. SEM results of catalysts

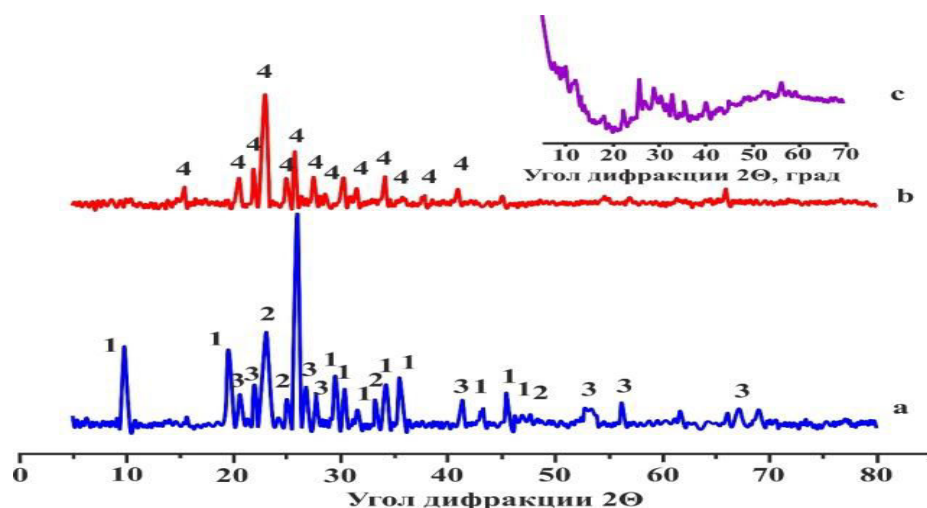
**Hydrothermal synthesis of iron molybdate.** Hydrothermal synthesis has long established itself as one of the most widespread methods for obtaining various functional nanomaterials with specified micro and nanostructures. He has demonstrated advantages in the processing of nanostructured materials for a variety of industries such as electronics, optoelectronics, catalysis, ceramics, magnetic storage, biomedicine, and biophotonics. The process of hydrothermal synthesis initiates the nucleation and growth of nanocrystals. In particular, the formation of crystalline products through a hydrothermal process can be performed at substantially lower temperatures than those required in solid-phase synthesis. Hydrothermal synthesis is regarded as one of the most promising due to such advantages as a relatively low reaction temperature and chemical homogeneity.

The method of hydrothermal synthesis makes it possible, under relatively mild conditions, to obtain nanocrystalline powders in one step with the ability to control the morphology, particle size, and phase composition of the products. Investigations of the process of hydrothermal synthesis of iron molybdate and, on its basis, a catalyst for the partial oxidation of methane to formaldehyde, we used ammonium heptamolybdate  $(\text{NH}_4)_6\text{Mo}_7\text{O}_{24}\cdot 4\text{H}_2\text{O}$  and iron nitrate  $\text{Fe}(\text{NO}_3)_3\cdot 9\text{H}_2\text{O}$ .

As the data of X-ray phase analysis show, the process of formation of a crystalline precipitate is significantly influenced not only by temperature but also by the duration of synthesis.

As a result of hydrothermal treatment (HTT) at a temperature of 100 °C for 4 hours, well-crystallized phases are formed (Figure 3). An increase in the HTT time to 8 hours leads to a strong amorphization of the product. Formation of this phase, which cannot be indexed as one of the known crystalline phases of iron molybdate (Figure 3).

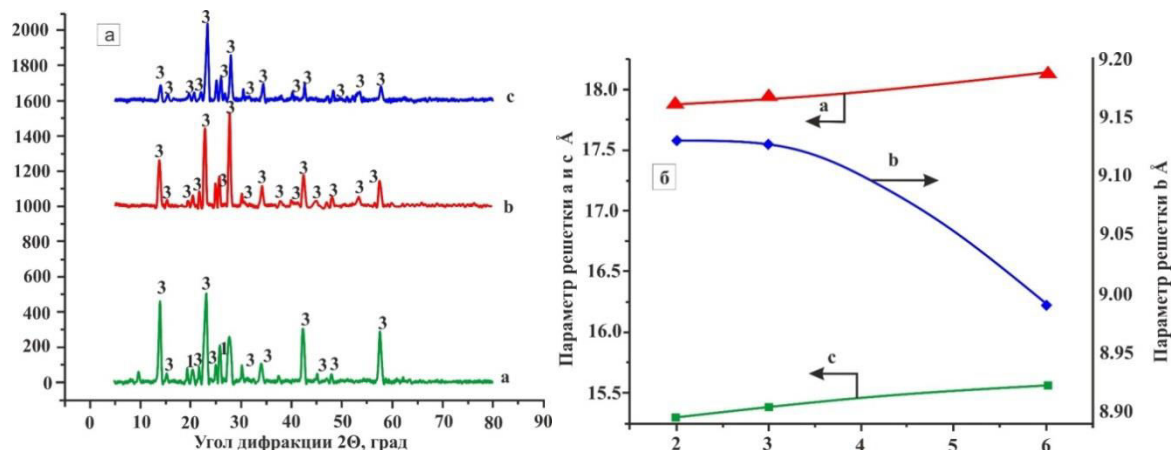
It crystallizes directly from the mother liquor as an intermediate product. Hydrothermal treatment for 10 hours at a temperature of 100 °C leads to an almost complete conversion of  $\text{Fe}_2(\text{MoO}_4)_3$  into iron molybdate (Figure 3).



Synthesis temperature 100 °C; indexing phase: 1- $\alpha$ - $\text{MoO}_3$ ; 2-NiO; 3- $\text{Co}_2\text{O}_3$ ; 4- $\text{NiO} \cdot \text{Co}_2\text{O}_3 \cdot \text{ZrO}_2 \cdot \text{Fe}_2(\text{MoO}_4)_3$ . a-3 hours; b-10 hours; s-15 hours

Figure 3. Changes in the radiograph during the hydrothermal synthesis of iron molybdate

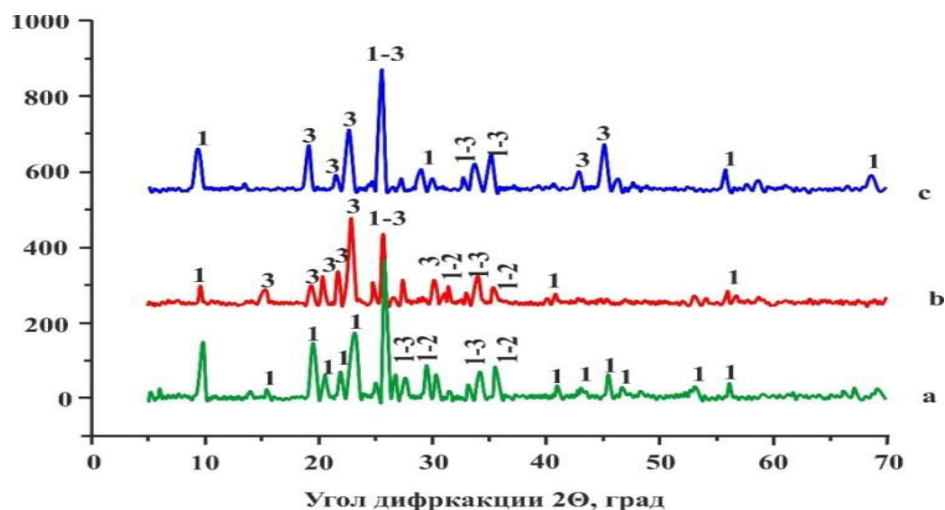
At ASTM International (American Society for Testing and Materials) there are numerous variations in the structures of iron molybdate. So, for example, there are two types of monoclinic crystal lattice  $\text{Fe}_2(\text{MoO}_4)_3$ , in which the position of the 100% peak differs significantly from  $2\theta = 22,99^\circ$  и  $2\theta = 27,51^\circ$ . The difference in the parameters of the crystal lattice a, b, and c is minimal and only the angle  $\beta$  differs insignificantly. Refinement of the parameters of the crystal lattice of iron molybdates obtained at different times of hydrothermal treatment indicates a rearrangement of the crystal lattice of iron molybdate. Only the lattice parameter b and the angle  $\beta$  undergo significant changes. An increase in temperature and, accordingly, pressure in the autoclave made it possible to establish that carrying out the process at a temperature of 160 °C and absolute pressure of 617 kPa for 3 hours, the interaction between the components of the mixture ends, as evidenced by the absence of free molybdenum oxide on the X-ray diffraction patterns (Figure 4).



Duration of hydrothermal treatment: a-2 hours; b-4 hours; at -8 o'clock indexing phase: 1-  $\text{MoO}_3$ ; 2- $\text{Fe}_2(\text{MoO}_4)_3$ .

Figure 4. Influence of hydrothermal treatment time on the phase composition (a) and structural parameters (b) of iron molybdate at 160 °C

Analysis of X-ray diffraction patterns shows that the formation of iron molybdate at a temperature of 160 °C is completely completed within 3 hours (Figure 4). However, the position of the 100% peak is significantly shifted compared to other samples. In this case, the starting materials, oxides or hydroxides of molybdenum and iron are not detected. Modelling the structure of iron molybdate indicates the possible existence of another iron molybdate, which has a monoclinic crystal lattice, differing from analogues only by the angle  $\beta=125,46^\circ$ . Thus, the hydrothermal process makes it possible to obtain monoclinic  $\text{Fe}_2(\text{MoO}_4)_3$  micron-sized particles with a complex three-dimensional structure.

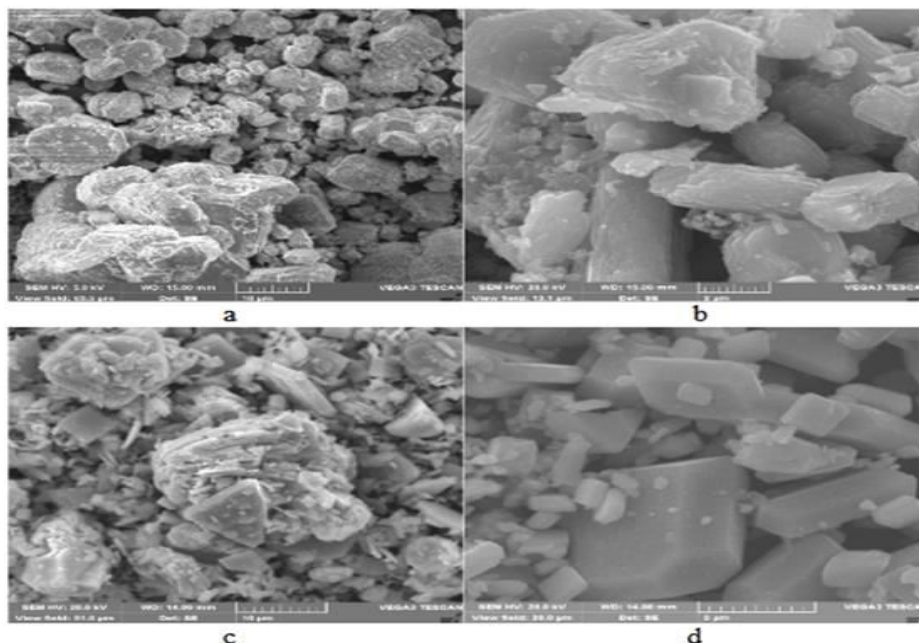


Hydrothermal treatment temperature: a-100 °C; b-150 °C; v-200 °C

Indexed phases: 1- $\text{MoO}_3$ ; 2- $\text{Fe}_2\text{O}_3$ ; 3- $\text{Fe}_2(\text{MoO}_4)_3$

Figure 5. The effect of temperature and pressure on the phase composition of iron molybdate at a duration of 3 h





Hydrothermal treatment temperature: 120 °C

Duration of hydrothermal treatment: 4 hours; Mo: Fe atomic ratios: a-1; b-1.5; s-2.0; d-2.3;

Figure 6. Hydrothermal synthesis of iron molybdate SEM results

Analyzing the results of scanning electron microscopy, it can be seen that Mo:Fe ratio significantly changes the shape and size of the particles (Figure 6). However, samples with a Mo:Fe ratio  $<2.1$  have a densely packed layered structure with a wafer thickness of about 500 nm. Note that a sample with a Mo: Fe = 2.1 ratios is distinguished by the predominance of particles of a regular, although not symmetric, shape. The particles can be characterized as a combination of simple forms of the monoclinic system: two pinacoids and four dihedrons. An increase in Mo:Fe atomic ratio to 2.5 leads to a chaotic arrangement of crystals of irregular shape combined into an aggregate with a hollow interior. These morphological changes observed above can be attributed to the difference in the process of crystallization and crystal growth under different reaction conditions.

## CONCLUSIONS

The analysis of the physicochemical and operational characteristics of two industrial catalysts for the synthesis of nanocarbon is carried out. Various methods: X-ray phase, chemical, IR spectroscopy investigated the composition of the catalysts. It was shown that the main component of industrial catalysts is iron molybdate (67.27%). The catalyst contains about 31%  $\text{MoO}_3$ , and 1-2% of molybdenum oxide is included in the lattice of iron molybdate, forming a solid solution. The presence of acid sites of the type on the surface of the catalysts was detected by IR spectroscopy. Lewis and Bronsted and the main centres of varying strength. The catalysts are highly active: their formaldehyde productivity reaches a value (12.5-13 mmol/g.s). The surface area of industrial contacts is (7-9  $\text{m}^2/\text{g}$ ); the size of the mesopores is 2-40 nm. Thus, industrial catalysts for the synthesis of nanocarbon are of high quality, which ensures their high performance throughout the entire period of operation.

**REFERENCES**

1. Bobomurodova, S. Y., Fayzullaev, N. I., & Usmanova, K. A. (2020). Catalytic aromatization of oil satellite gases. *International Journal of Advanced Science and Technology*, 29(5), 3031-3039.
2. Tursunova, N. S., & Fayzullaev, N. I. (2020). Kinetics of the Reaction of Oxidative Dimerization of Methane. *International Journal of Control and Automation*, 13(2), 440-446.
3. Fayzullaev, N. I., Bobomurodova, S. Y., Avalboev, G. A., Matchanova, M. B., & Norqulova, Z. T. (2020). Catalytic Change of C1-C4-Alkanes. *International Journal of Control and Automation*, 13(2), 827-835.
4. Mamadoliev, I. I., Khalikov, K. M., & Fayzullaev, N. I. (2020). Synthesis of high silicon of zeolites and their sorption properties. *International Journal of Control and Automation*, 13(2), 703-709.
5. Sarimsakova, N. S., Atamirzayeva, S. T., Fayzullaev, N. I., Musulmonov, N. X., & Ibodullayeva, M. N. (2020). Kinetics and mechanism of reaction for producing ethyl acetate from acetic acid. *International Journal of Control and Automation*, 13(2), 373-382.
6. Mamadoliev, I. I., & Fayzullaev, N. I. (2020). Optimization of the activation conditions of high silicon zeolite. *International Journal of Advanced Science and Technology*, 29(03), 6807-6813.
7. Omanov, B. S., Xatamova, M. S., Fayzullaev, N. I., Musulmonov, N. K., & Asrorov, D. A. (2020). Optimization of vinyl acetate synthesis process. *International Journal of Control and Automation*, 13(1), 231-238.
8. Ibodullayevich, F. N., Yunusovna, B. S., & Anvarovna, X. D. (2020). Physico-chemical and texture characteristics of Zn-Zr/VKTS catalyst. *Journal of Critical Reviews*, 7(7), 917-920.
9. Omanov, B. S., Fayzullaev, N. I., & Xatamova, M. S. (2020). Vinyl Acetate Production Technology. *International Journal of Advanced Science and Technology*, 29(3), 4923-4930.
10. Fayzullayev, N. I., & Umirzakov, R. R. (2005). To obtain acetone by spontaneous hydration of acetylene. In *ACS National Meeting Book of Abstracts* (pp. PETR-71).
11. Fayzullayev, N. I., Umirzakov, R. R., & Pardeaeva, S. B. (2005). Study of acetylating reaction of acetylene by gas chromatographic method. In *ACS National Meeting Book of Abstracts* (pp. PETR-66).
12. Fayzullaev, N. I., Jumanazarov, R. B., & Turabjanov, S. M. (2015). Heterogeneous Catalytic Synthesis of Vinylchloride by Hydrochlorination of Acetylene. *IJSET-International Journal of Innovative Science, Engineering & Technology*, 2(9).
13. Fayzullaev, N.I., Fayzullaev, O.O. Kinetic regularities in reaction of the oxidizing condensation of methane on applied oxide catalysts//*Khimicheskaya Promyshlennost'*, 2004, (4), стр. 204–207
14. Fayzullaev, N.I., Muradov, K.M. Investigation of reaction of catalytic vapor-phase synthesis of vinyl acetate on applied catalyst//*Khimicheskaya Promyshlennost'*, 2004, (3), стр. 136–139

15. Mukhamadiev, N.Q., Sayitkulov, Sh.M., Ergashev, I.M., Khafizov, Kh.F., Fayzullaev, N.I. Optimization of separation on the basis of Unifac parameters and evaluation of the composition of the stationary phase in gas-liquid chromatography//*Chromatographia*, 2003, 57(11-12), стр. 831–833
16. Muradov, K.M., Fajzullaev, N.I. Technology for producing the ethylene using the reaction of the oxidizing condensation of methane//*Khimicheskaya Promyshlennost'*, 2003, (6), стр. 3–7
17. Muradov, K.M., Fajzullaev, N.I. Optimization of process of synthesis of aromatic nitriles//*Khimicheskaya Promyshlennost'*, 2003, (4), стр. 8–11
18. Muradov, K.M., Fajzullaev, N.I. Optimization of process of synthesis of aliphatic nitriles//*Khimicheskaya Promyshlennost'*, 2003, (3), стр. 3–10
19. Fayzullaev, N. I., Yusupov, D., Shirinov, X. S., Korotoev, A. V., & Umirzakov, R. R. (2002). Catalytic vaporphase hydration of acetylene and its derivatives. *Chemical Industry. N, 7*, 1-33.
20. Chorievich Aslanov, S., Qobilovich Buxorov, A., & Ibodullaevich Fayzullayev, N. (2021). Catalytic synthesis of C<sub>2</sub>-C<sub>4</sub>-alkenes from dimethyl ether. *arXiv e-prints*, arXiv-2104.
21. Khamroev, J. X., Fayzullaev, N. I., & Haydarov, G. (2021). Texture Characteristics of Modified and Activated Bentonite. *Annals of the Romanian Society for Cell Biology*, 12160-12174.
22. Kh, K. J., Fayzullaev, N. I., Sh, K. G., Temirov, F. N., & Kh, J. M. (2021). Texture and Sorption Characteristics of Bentonite-Based Sorbents. *Annals of the Romanian Society for Cell Biology*, 828-849.
23. Temirov, F. N., Fayzullaev, N. I., Khaidarov, G. S., Khamroev, J. K., & Jalilov, M. K. (2021). Optimization of the Process Acid Activation of Bentonite. *Annals of the Romanian Society for Cell Biology*, 809-827.
24. Temirov, F. N., Fayzullaev, N. I., & Haydarov, G. (2021). Texture and Sorption Characteristics of Modified Bentonite Made by Ash-Gel and Together Equipment. *Annals of the Romanian Society for Cell Biology*, 12175-12185.